Analysis Report on Sample RN-1-2010

Report Author: Steve Colbern

16 July, 2011

© 2011 by S. G. Colbern-All Rights Reserved

Background Information

Location of Object: Inner portion of right wrist. The object showed up easily on a medical X-ray.

The subject, Mr. Ron Noel, believes that the object may have been inserted during a remembered alien contact experience in 1969, in which he was abducted along with two friends.

Tests Done With the Object in the Subject's Body: The object was located on a medical X-ray, on which it showed up easily.

The object was then scanned, using a studfinder, which gave a strong signal when over the object, indicating it was composed of metal, or other electrically conductive material.

The object was then scanned with a Gaussmeter, which measured a magnetic field over the object of approximately 7 mGauss, indicating that the object was made of magnetic material, and emitting a magnetic field.

The object was then scanned with a radio frequency detection instrument, which detected radio signals emitted at 137.72926 MHz and 516.812 GHz frequencies.

Appearance and Physical Characteristics of Sample

Type of Membrane around Object: Appeared to be composed of normal tissue; was not black, or difficult to cut through. Numerous vesicles, which appeared to be filled with yellowish oil were embedded in the membrane, however.

Type and Characteristics of main Object: Seed-shaped, ~3 mm X 2 mm X 1 mm; similar to at least two other objects that were also taken from the wrists of abductees.

Analytical Procedure

The object was removed surgically on April 24, 2009, by Dr. Roger Leir, imaged briefly under a dissecting microscope, and stored in a tube of the patient's blood serum immediately thereafter, exposed to the field of a neodymium-iron-boron (NIB) magnet, to determine if it was ferromagnetic. The object was then stored in a refrigerator.

The sample was then subjected to light microscopy, at low magnification. The internal, X-ray dense object was dissected out of its surrounding tissue capsule, and observed under higher magnification.

The sample was then given an initial test by scanning electron microscopy (SEM), and energy dispersive X-ray (EDX) elemental analysis. An attempt was then made to cut the object in half to get SEM images of the interior.

The object was extremely hard, had extremely high mechanical strength, and proved impossible to cut, even with diamond tools. It was then cut in half, using a high-power, pulsed, laser. The interior and exterior surfaces of the object were then scanned more extensively by SEM and EDX.

Half of the object was then analyzed by inductively coupled plasma mass spectrometry (ICP-MS), in order to quantitatively determine the concentrations of all elements in the sample.

The tissue capsule surrounding the object was then dried in a vacuum dessicator and analyzed by Fourier Transform Infared Spectroscopy (FTIR) to determine the composition of the oil which was seen in the tissue.

Analysis Results

Light Microscopy

The object is shown in Figures 1 and 2, at 10X and 20X magnification, just after removal from Mr. Noel. The outer layer of the object was a capsule of tissue, resembling epithelial tissue, which clung tightly to the metallic core. Numerous small vesicles or what appeared to be a yellow liquid were evident in the tissue layer.

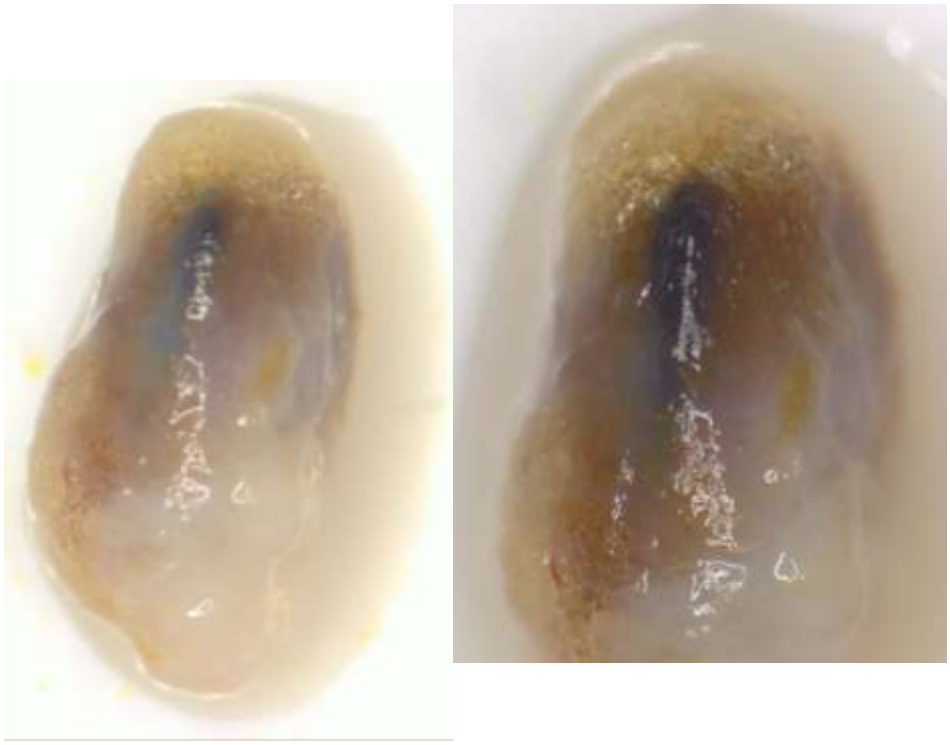

Figures 1 and 2-Object in Tissue Capsule just after Removal-10X Magnification (left) and 20X (right)

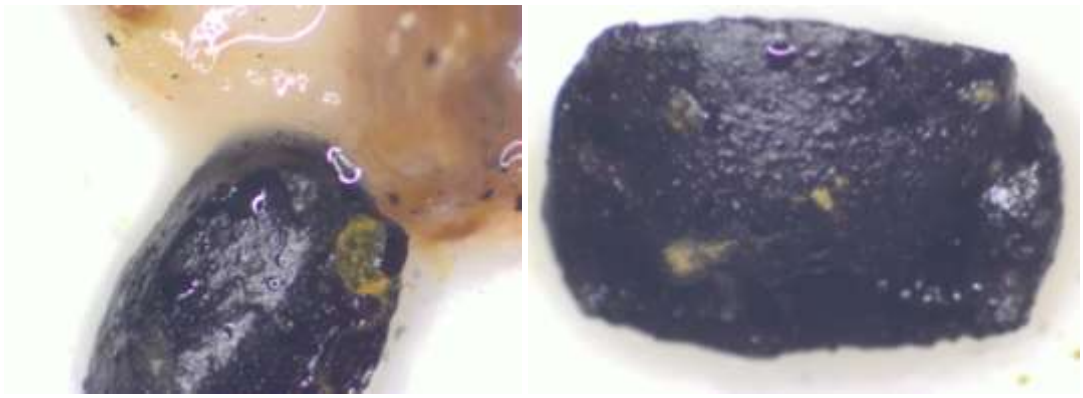

Figures 3 and 4-Object after Removal from Tissue Capsule-20X Magnification

Small nerve fibers were seen connecting to the tissue surrounding the object in the initial dissecting microscope images.

The tissue capsule was quite different from the grey, electrically conductive, membrane surrounding most of the other implants removed from patients by Dr. Leir, but a similar structure was observed previously in one other implant case.

After careful dissection of the metallic core from the tissue capsule, the core was imaged at various magnifications (Figures 3-12). The core proved to be covered with a shiny, black coating, which appeared very similar to the coating on the implant removed from patient "John Smith" in removal case #15.

The coating on the sample showed many small, regular pits under high magnification (Figures 12 and 13). These pits appeared to go through the coating, to contact the metal underneath. The coating also had a uniform, bumpy texture, visible under high magnification, which appeared unusual (Figures 11 and 12).

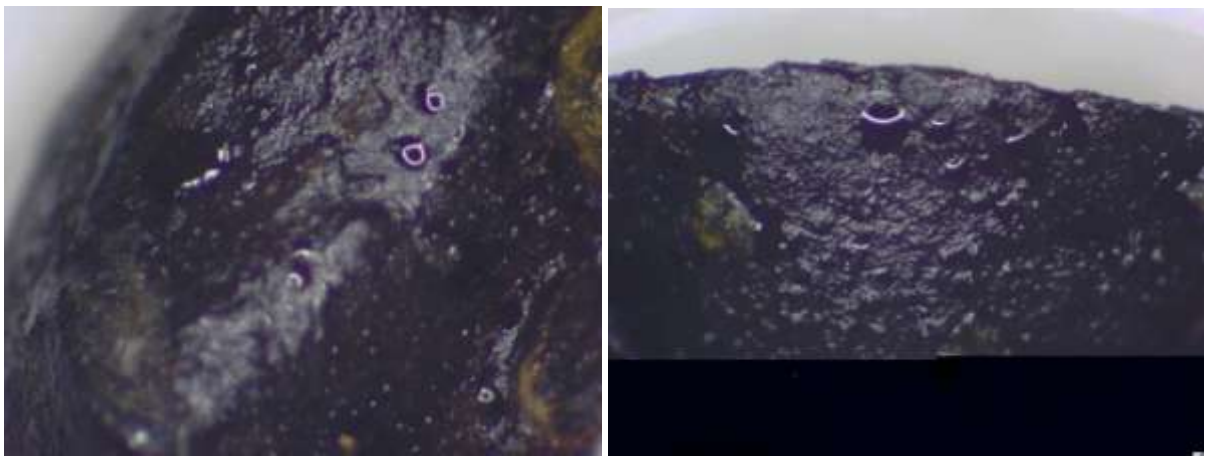

Figures 5 and 6-Object after Removal from Tissue Capsule-40X Magnification

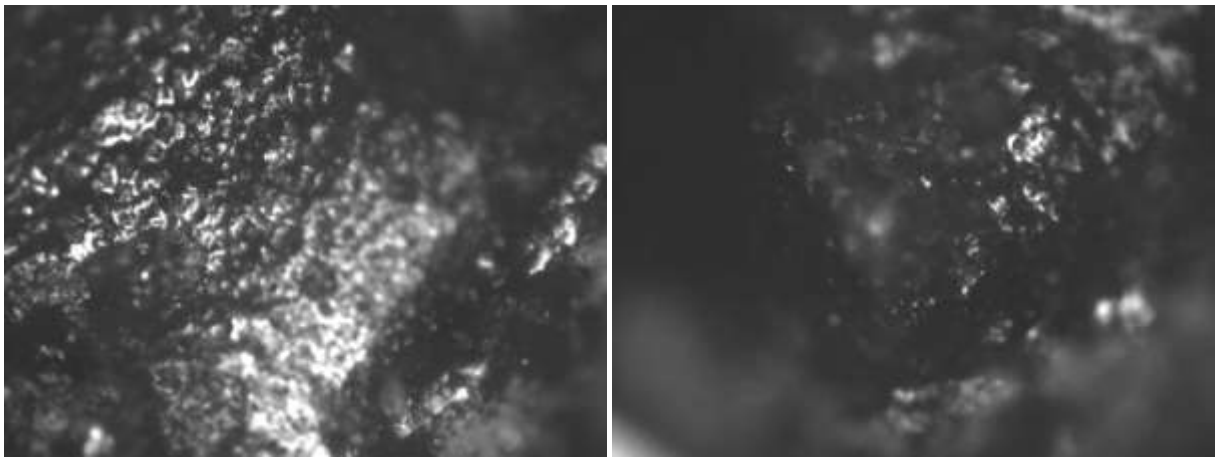

Figures 7 and 8-Object after Removal from Tissue Capsule-100X Magnification

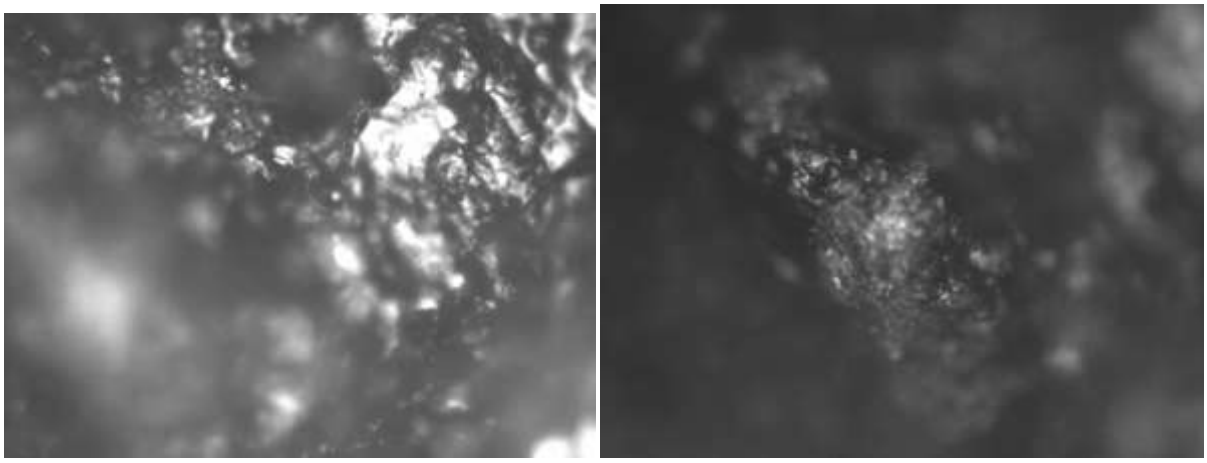

Figures 9 and 10-Object after Removal from Tissue Capsule-200X Magnification

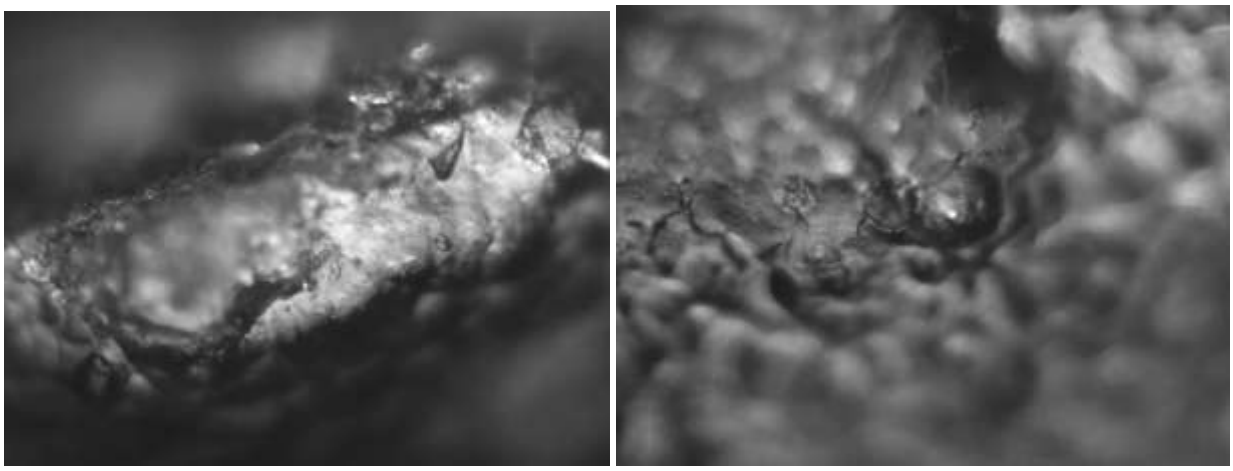

Figures 11 and 12-Object after Removal from Tissue Capsule-500X Magnification

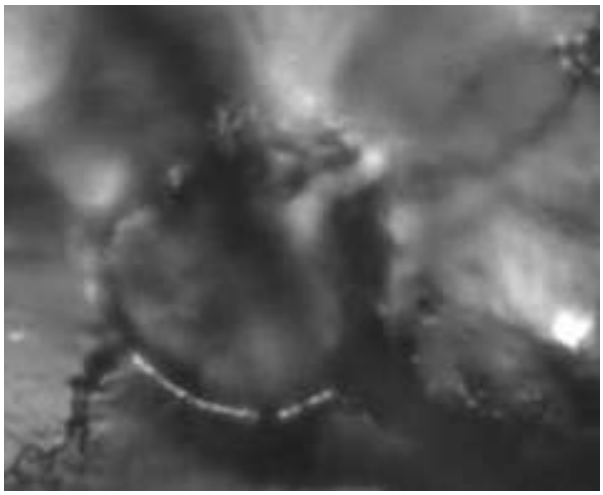

Figure 13-Close-Up View of Pit in Object Coating

SEM Imaging

Low magnification SEM images are shown in Figures 14 and 15. The entire object is shown in Figure 14, before cutting, and half of the object is shown, after laser cutting, in Figure 15. Fibers, and the pitted coating on the metal, are evident in both of these images.

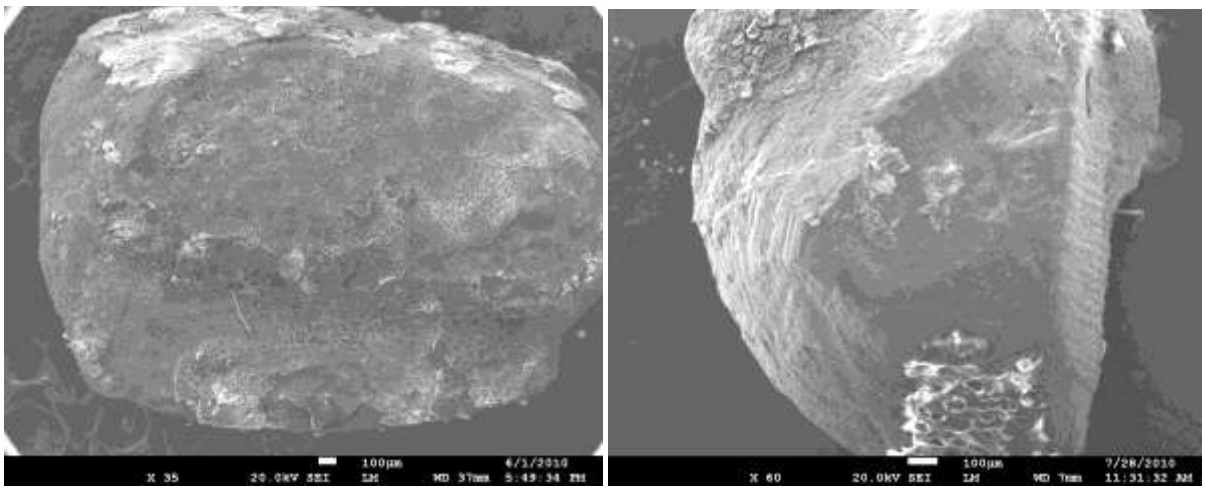

Figures 14 and 15-Entire Metallic Portion of Object (35X, Left) and Half of Object after Laser Cutting (60X, Right)

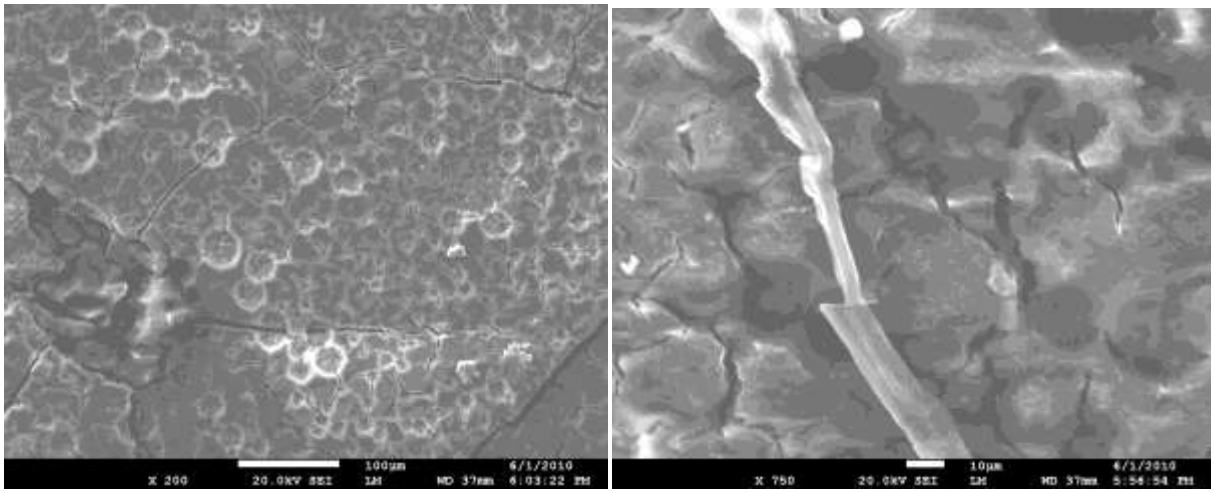

Figures 16 and 17-Object Coating-Showing Pits and Linear Structure (750X-800X)

Somewhat higher magnification (200X-750X) images of the coating and fibers are shown in Figures 16 and 17. The rough texture and pits in the coating are very evident in these two images.

A close up (3500X) of one of the pits is shown in Figure 18, where it was observed that the pits appear to go all the way through the coating to the metal surface underneath. Each pit had fairly regularly spaced cracks radiating from the centers, and most had a central structure, spherical, or cylindrical in shape, which appeared to be part of the metal surface.

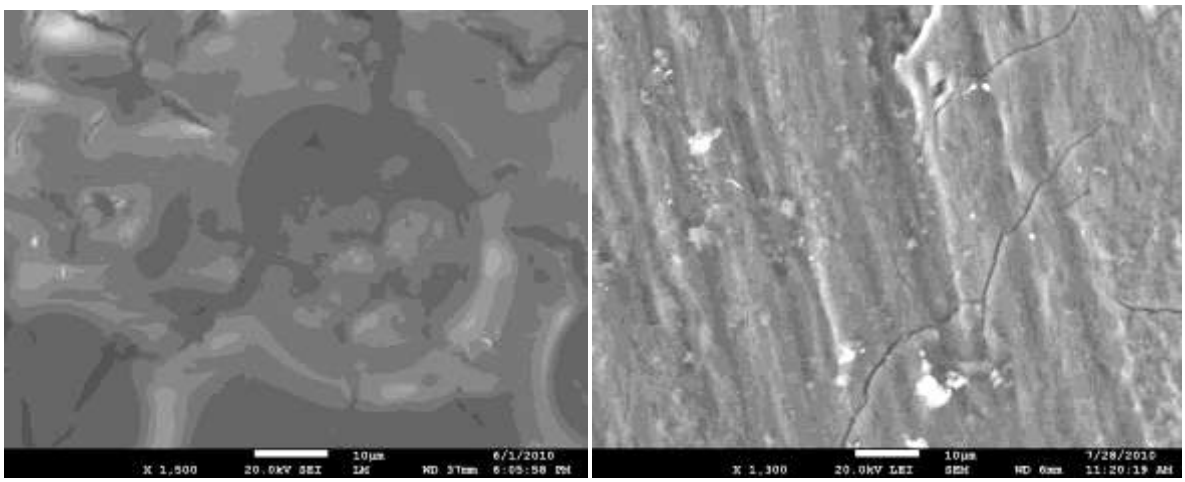

Figures 18 and 19-Close-Up of Pit and Grooves and Cracks in Coating (1300X-1500X)

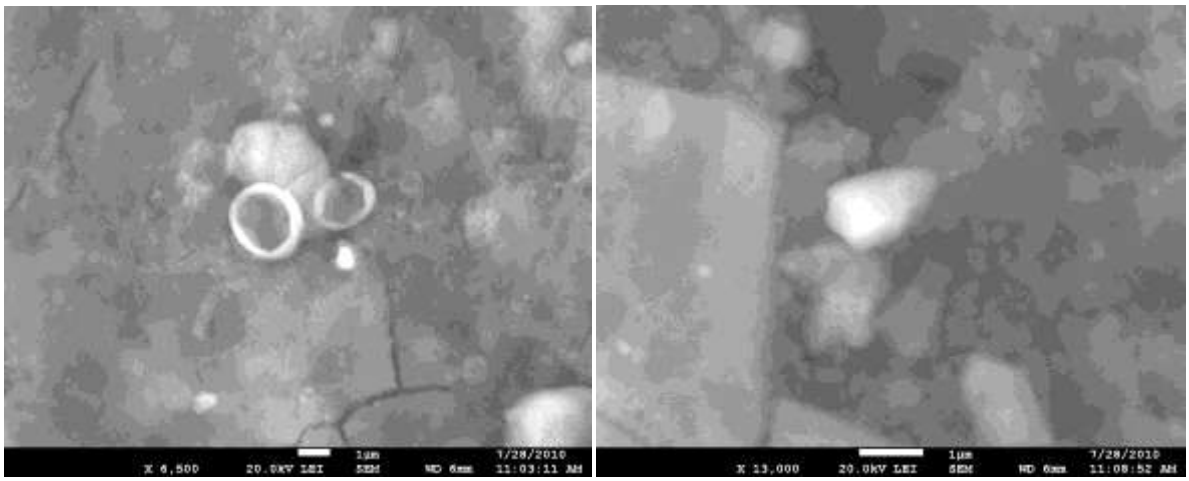

Figures 20 and 21-Odd Circular Structures and Loose Chunks in Coating (6500X-13000X)

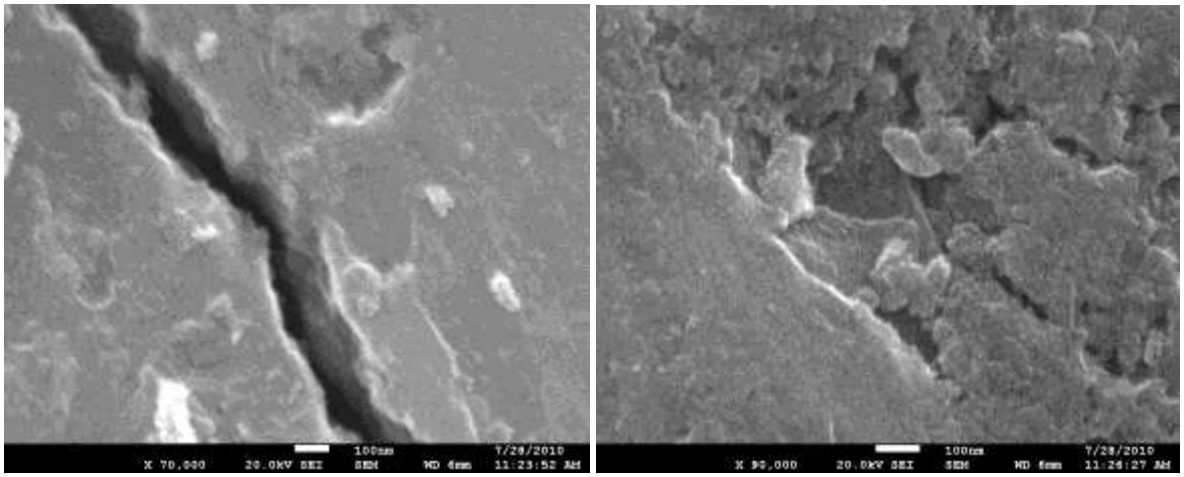

Figures 22 and 23-High-Magnification Images of Crack in Coating and Bare Metal Surface (70000X-90000X)

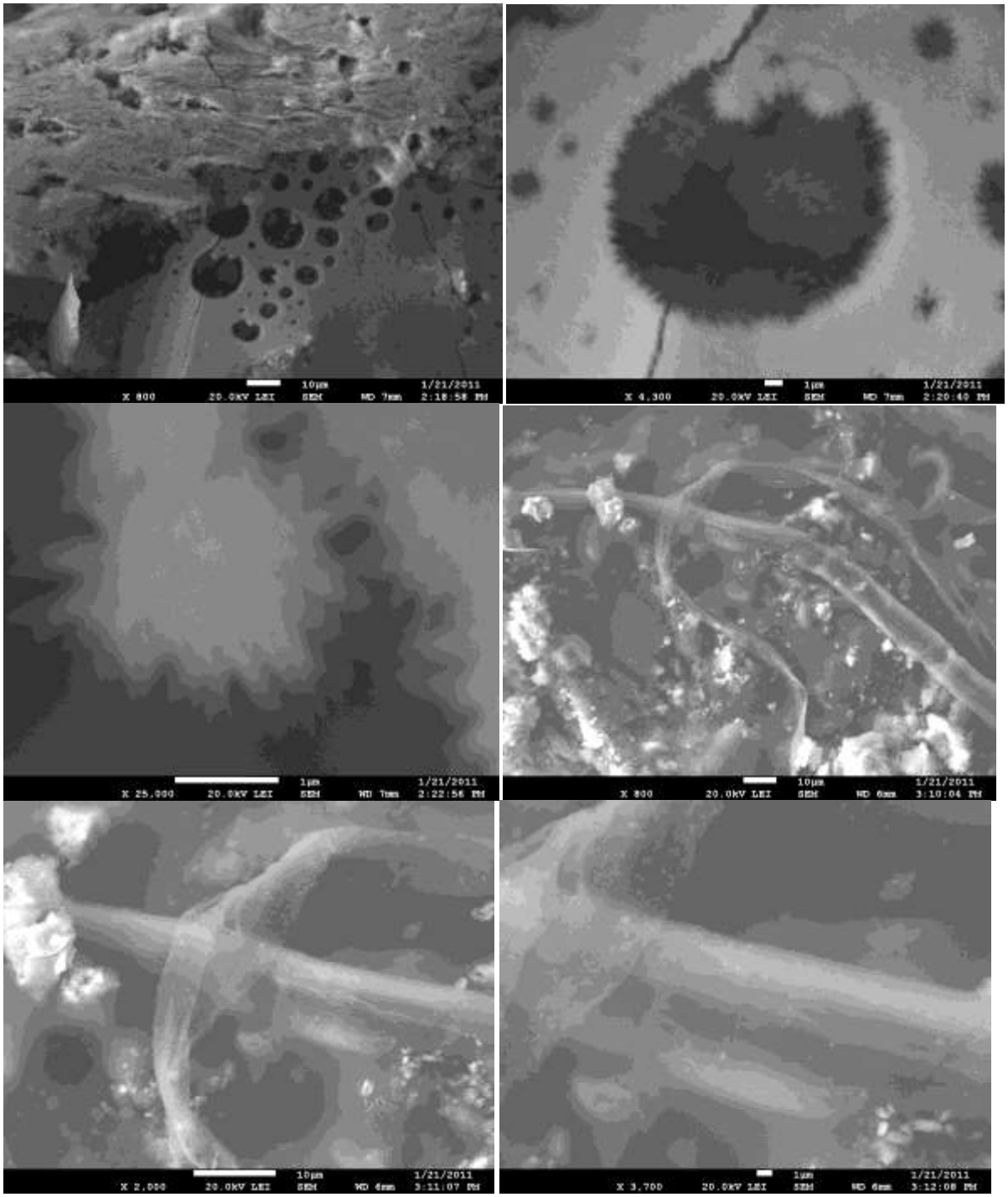

Figures 24-29-Images of Acid-Treated Half of Object-Showing Perforated Structures, Nanofibers and Microtubes

Some areas of the coating showed grooves (Figure 19). These grooves were very regularly spaced, approximately 10 um apart.

Unusual circular structures were observed on one area of the samples coating (Figure 20). These structures were approximately 2.5 um in diameter. Loose chunks of material ranging from l um-10 um in largest dimension were also observed in some areas (Figure 21). The coating appeared to be broken up in these areas.

Higher magnification (70,000X) images of the coating showed a relatively smooth surface in the intact sections of coating, with some microcracks. Some small grains, which were 50 um-100 um in largest dimension were observed in the bare metal (laser cut) portion of the sample (Figures 22 and 23).

Images at magnifications higher than 90,000X could not be obtained due to focusing problems. These focusing problems with the instrument were not encountered with other samples imaged on the same day.

The half of the object which was treated with nitric/hydrochloric acid mixture in the course of the ICP-MS analysis was also imaged (Figures 24-29). The object was sufficiently acid resistant so that only the surface metal appeared to be etched away, and a more acid resistant material left behind.

This material appeared to consist of nano and micro tubules, some of which were formed into sheets having a complex, perforated structure. The openings in the perforated structure were of approximately the same size as the pits in the coating of the object, imaged earlier. EDX mapping data indicated that the microtubules were composed mainly of carbon (see EDX section).

EDX Data

The energy dispersive X-ray (EDX) elemental analysis of the surface of the coating of the object detected 11 elements (Figures 30 and 31). These were (in approximate order of abundance) iron (Fe), oxygen (O), phosphorus (P), carbon (C), sulfur (S), aluminum (Al), silicon (Si), calcium (Ca), chromium (Cr), chlorine (Cl), and potassium (K).

EDX point-and-shoot data on some of the structures seen on the surface of the coating revealed a very similar composition to that of the bulk composition of the coating. The only significant differences in the composition of the structures from that of the bulk coating were a somewhat higher concentration of calcium, the presence of manganese (Figure 32), and an increased concentration of chlorine (Figure 33).

EDX mapping data revealed a very uniform distribution of elements in the coating (see Appendix).

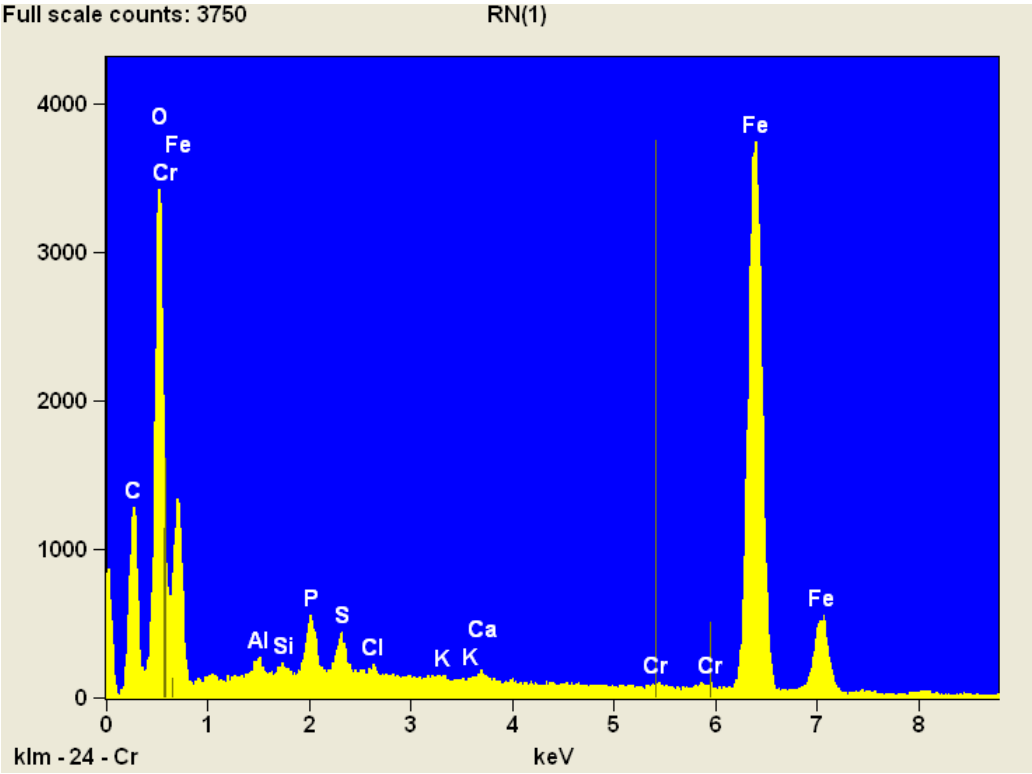

Figure 30-EDX Elemental Analysis Data from Coating of Ron Noel Object-Area 1

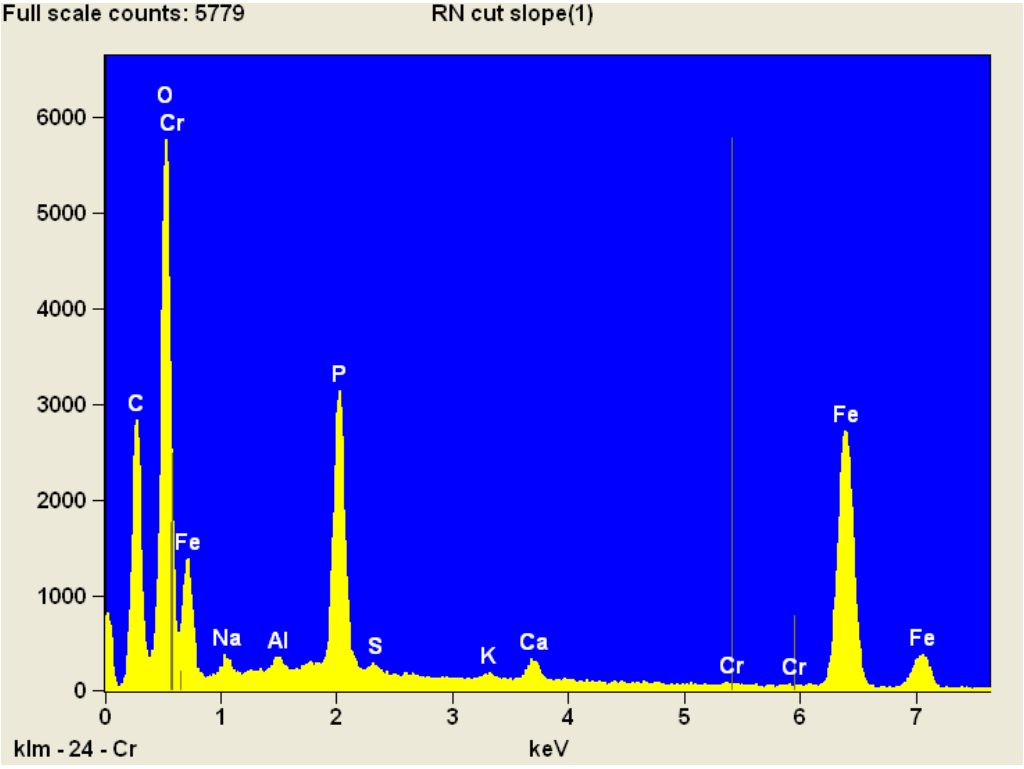

Figure 31-EDX Elemental Analysis Data from Coating of Ron Noel Object-Area 2

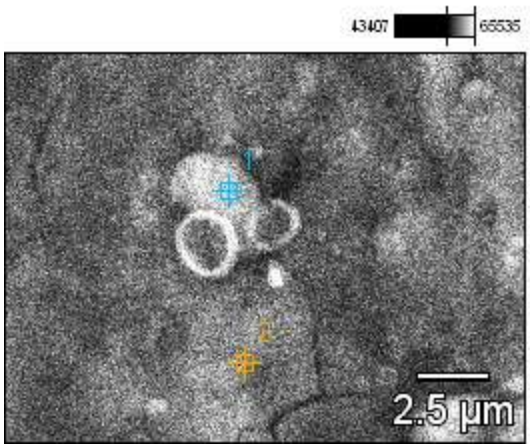

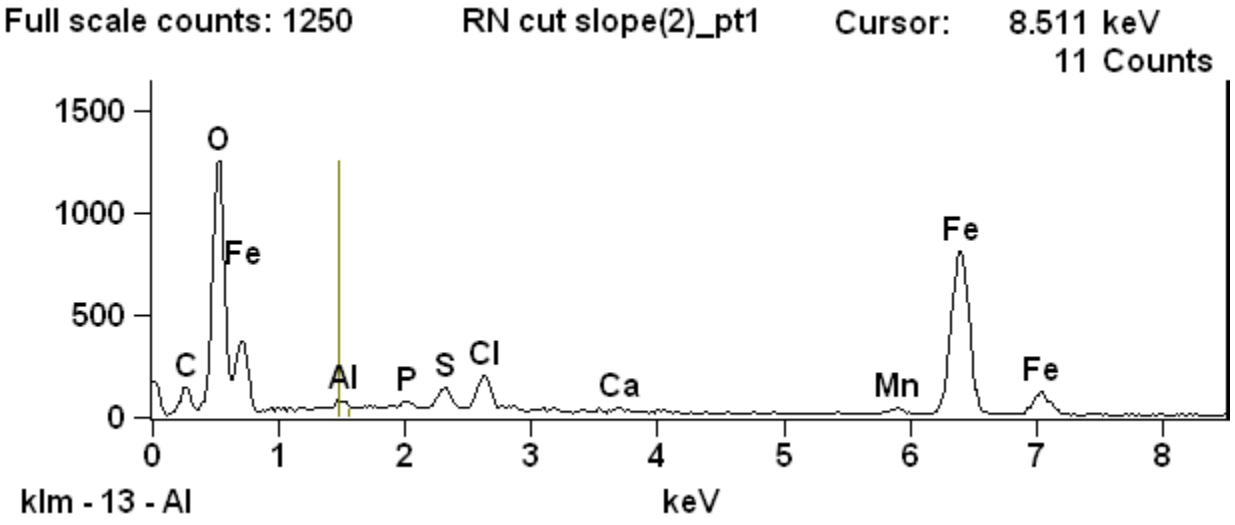

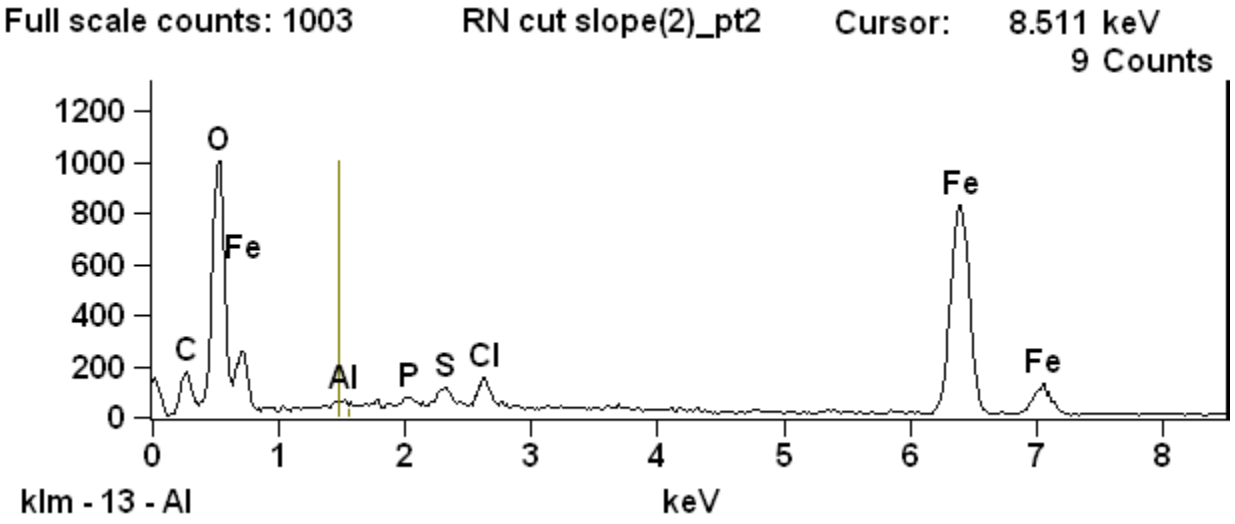

Figure 32-EDX Point and Shoot Data for Circular Structures and Nearby Coating

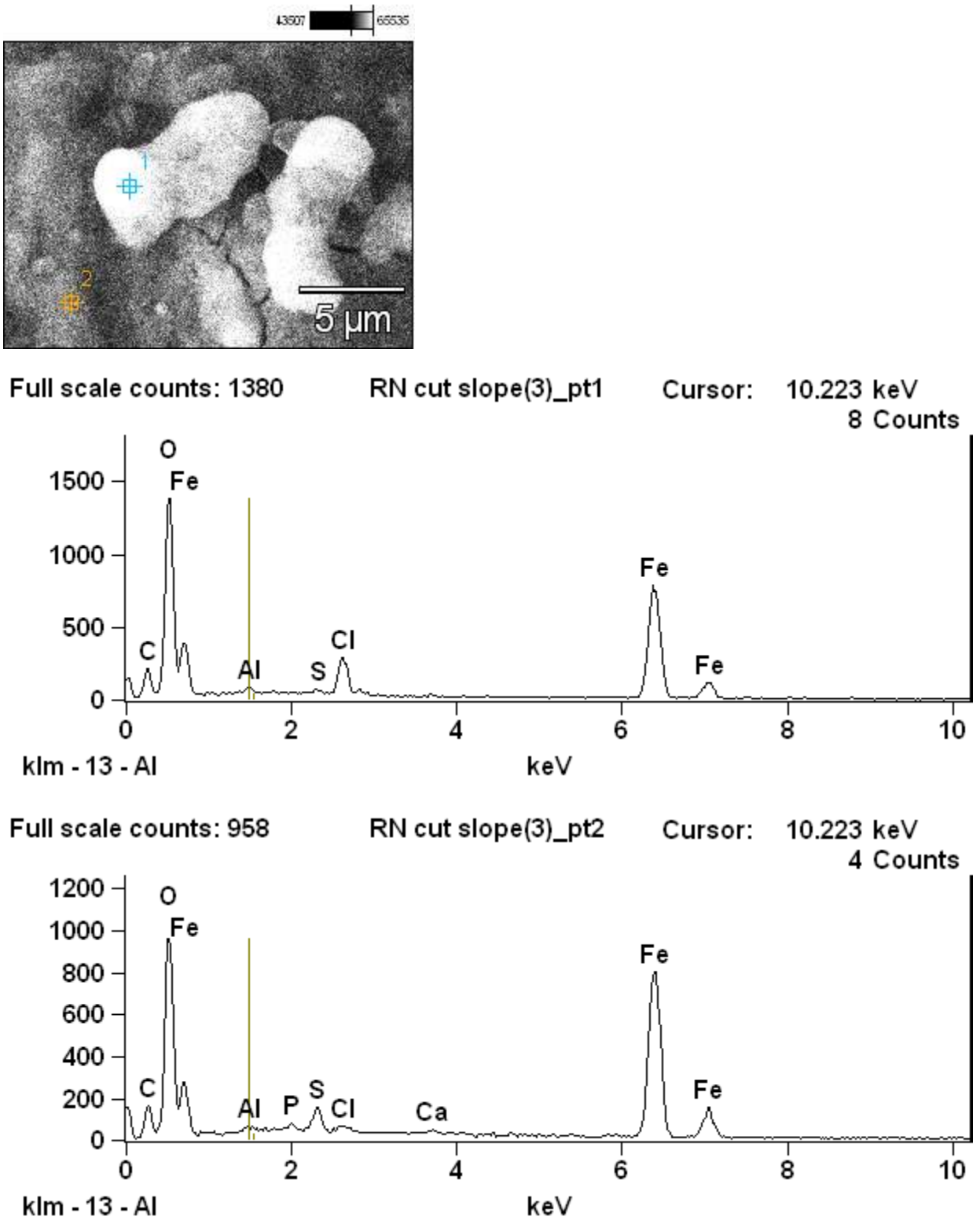

Figure 33-EDX Point and Shoot Data for Coating Structures and Nearby Coating

Magnetic and Electrical Analysis

The object was emitting a magnetic field with a strength of approximately 7 milliGauss (mGa) before removal from Mr. Noel.

The magnetic field decayed significantly within days of removal, and had decreased in intensity to less than 1 mGa 2 weeks after removal. The metallic portion of the object was also strongly attracted to a Neodymium-Iron-Boron (NIB) magnet.

The object was also emitting radio frequencies before removal; the emitted frequencies were determined to be 137.72926 Megahertz (MHz) and 516.812 Gigahertz (GHz).

Raman Spectroscopy

Raman spectroscopy, using 532 nm excitation laser wavelength, showed a strong luminescence signal, which is seen as the rise in intensity in the fullscale spectrum (Figure 34), along with a series of peaks from 100 cm^{-1}-450 cm^{-1} and two peaks at 1391 cm^{-1} and 1560 cm^{-1}.

These peaks strongly resemble the radial breathing mode (RBM) peaks and D-Band and G-Band peaks observed in commercial samples of single-walled carbon nanotubes (SWCNT) (Figures 35 and 36)[1].

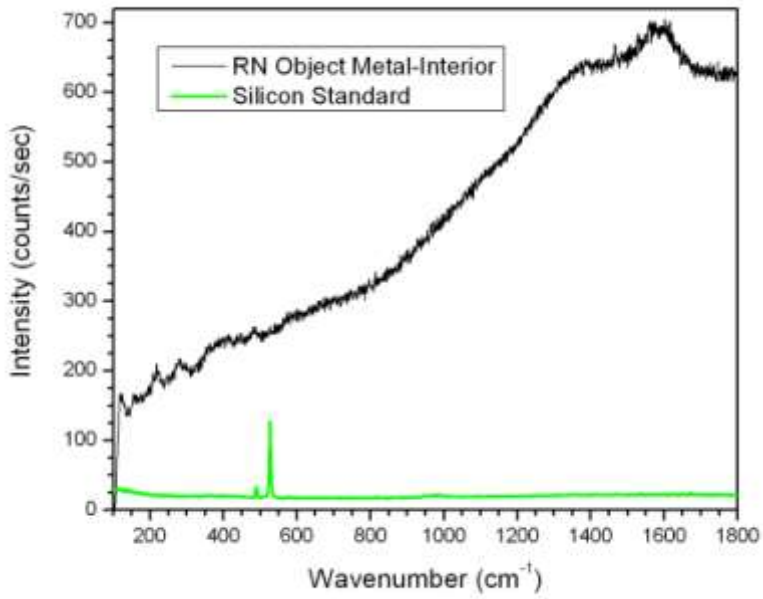

Figure 34-532 nm Raman Spectra of Interior of Metallic Portion of Ron Noel Object and Silicon Standard-Fullscale

[1] The G and D SWCNT bands are caused by C-C stretch of sp2 and sp3 hybridized carbon, respectively, while the RBM bands are caused by radial stretch of the entire SWCNT. SWCNT of different diameters give rise to different RBM band peaks.

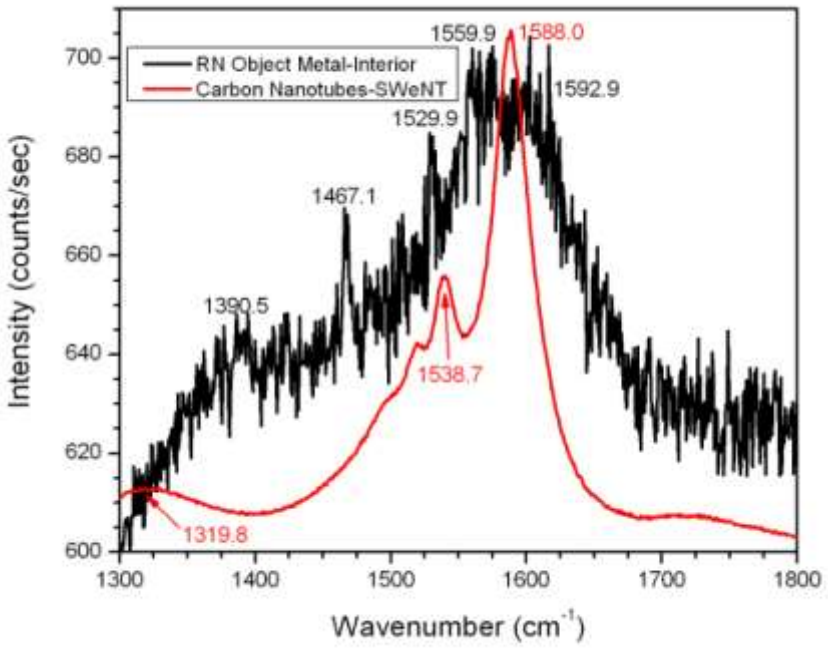

Figure 35-532 nm Raman Spectra of Interior of Metallic Portion of Ron Noel Object and Commercially Available Small-Diameter Single-Walled Carbon Nanotubes-D and G Bands

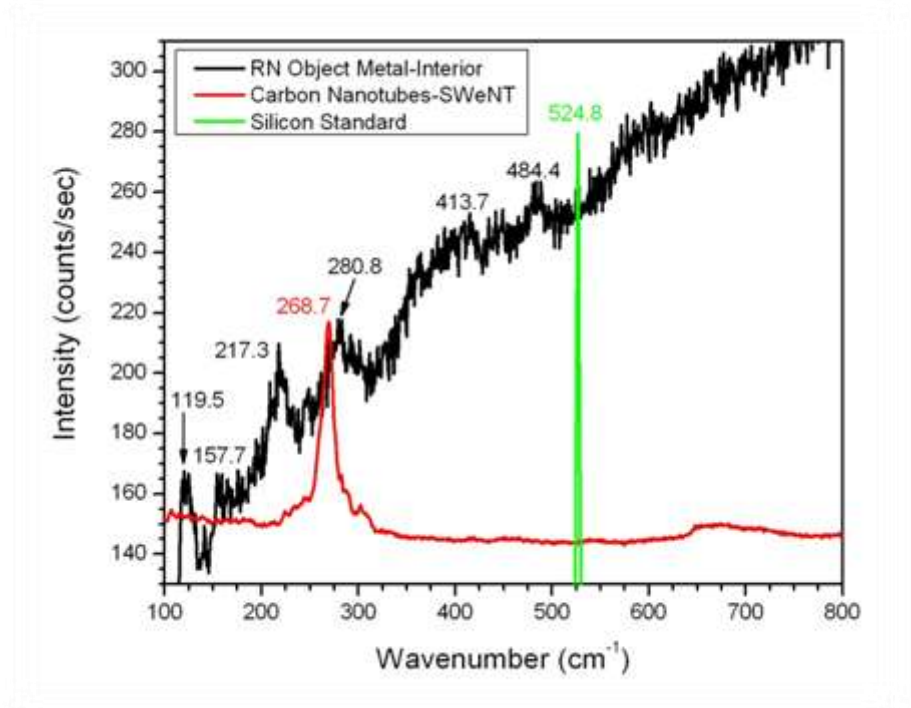

Figure 36-532 nm Raman Spectra of Interior of Metallic Portion of Ron Noel Object and Commercially Available Small-Diameter Single-Walled Carbon Nanotubes-RBM Band

The G and D band SWCNT peaks from the object are of somewhat higher wave-number than the commercial SWCNT (1592.9 cm^{-1}, vs. 1588.0 cm^{-1} for G-Band and 1390.5 cm^{-1} vs. 1319.8 cm^{-1} for D-Band), indicating a smaller average SWCNT diameter (Figure 35).

There are six radial breathing mode peaks from the sample, indicating that there are six types of SWCNT, with diameters of 2.00 nm, 1.54 nm, 1.12 nm, 0.87 nm, 0.59 nm, and 0.50 nm (Figure 36). The last two SWCNT in this group are of significantly smaller diameter than commercially available SWCNT, and are near the theoretical limit for smallest SWCNT diameter (~0.45 nm).

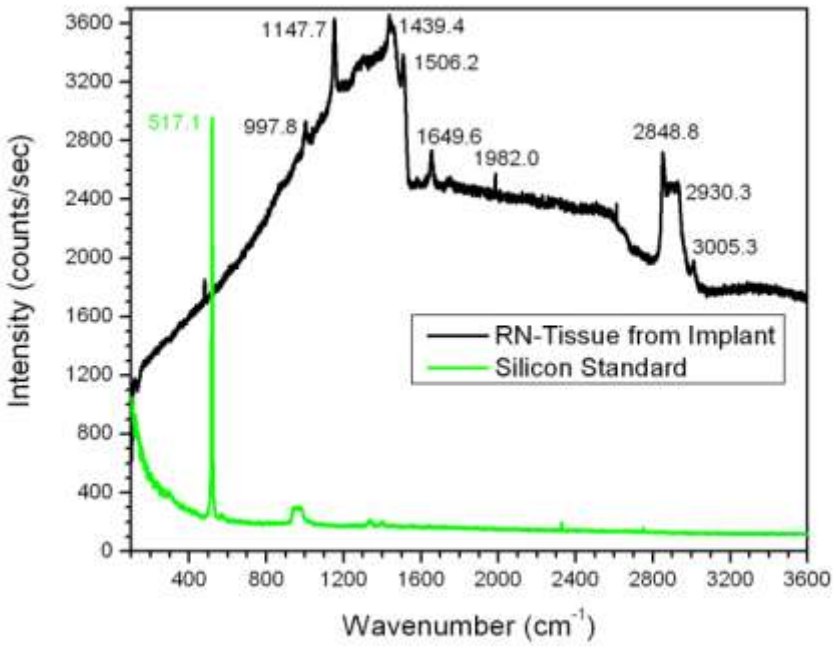

Figure 37-532 nm Raman Spectra of Tissue Covering of Ron Noel Object and Silicon Standard-Fullscale

The Raman spectrum of the dried tissue capsule surrounding the object is shown in Figure 37. The peaks observed from 3005 cm^{-1} to 2849 cm^{-1} are caused by hydrocarbon C-H bond stretching vibrations.

The small peak at 1649.6 cm-1 is caused by C=O, or unsaturated (double-bonded) C=C stretching vibrations. The broad peak at 1500 cm^{-1}-1140 cm^{-1} is caused by lower-energy CH_2 bending vibrations.

FTIR Analysis

The FTIR spectrum of the dried tissue surrounding the object is shown in Figure 38. The FTIR spectrum shows many of the same molecular vibrations as the Raman spectrum of the tissue capsule around the object (Figure 37).

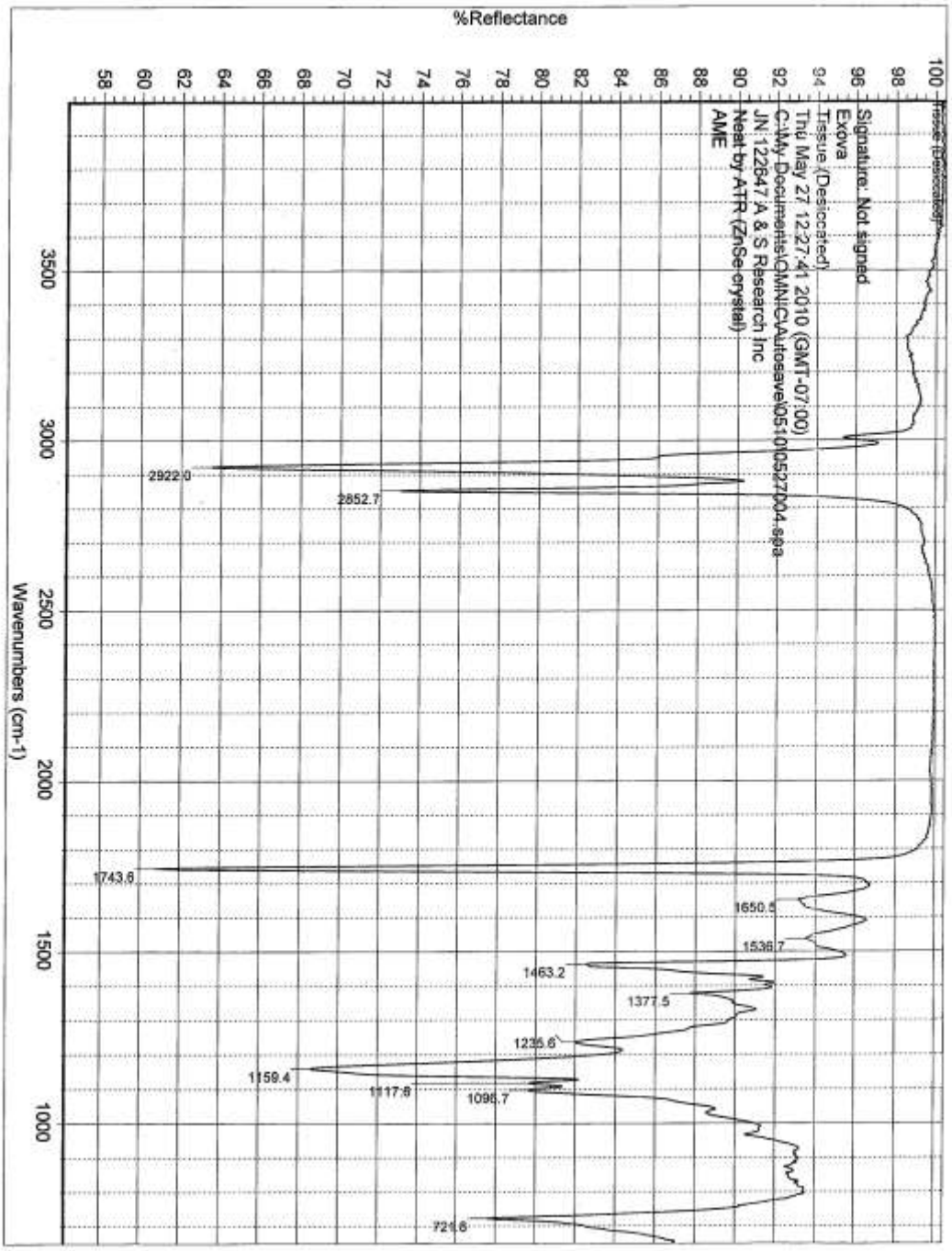

Figure 38-FTIR Spectrum of Dried Tissue Covering Metallic Portion of Ron Noel Object

The large peaks at 2922.0 cm^{-1} and 2852.7 cm^{-1} are also caused by C-H stretching vibrations. The intense peak at 1743.6 cm^{-1} is caused by carboxylate C=O stretch which was far smaller in the Raman spectrum of the tissue.

The small peak at 1650.5 cm^{-1} is caused by C=C stretch. As with the Raman spectrum, the peaks lower than 1500 cm^{-1} are caused by CH_2 stretching vibrations.

Both the FTIR and Raman spectra of the tissue capsule are consistent with that to be expected from the presence of esters with a long hydrocarbon chain, and few unsaturated carbons.

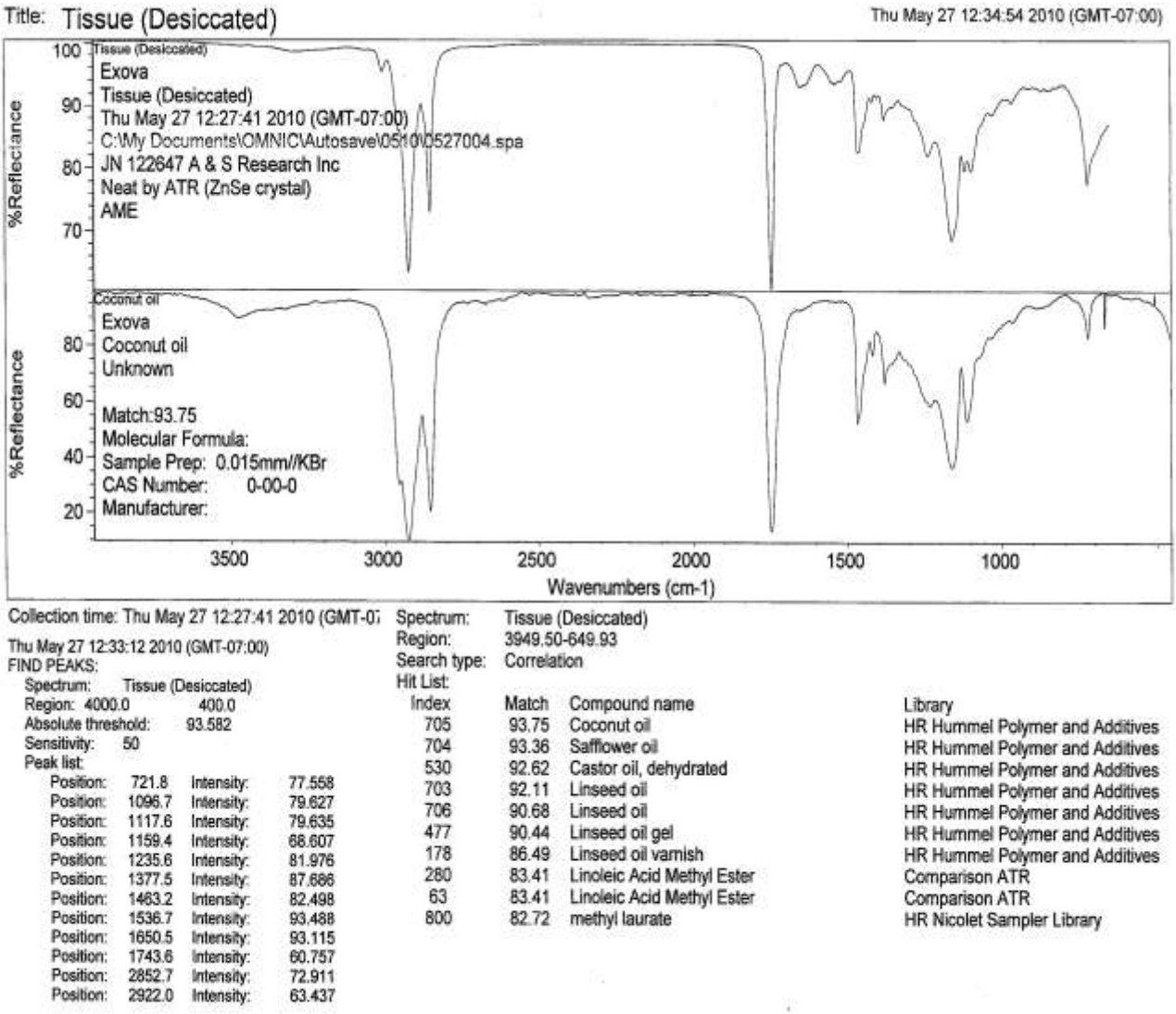

Figure 39-Comparison of FTIR Spectra of Dried Tissue Covering Metallic Portion of Ron Noel Object and Coconut Oil

The computer database of the FTIR instrument confirmed this hypothesis, with the best spectral match to the sample in the database being coconut oil, which is a glycerol tri-ester (fat) with a high percentage of lauric acid (Figure 39).

ICP-MS Analysis

The ICP-MS trace element analysis and sample preparation conditions for the metallic portion of the sample are shown in Figure 40.

Trace Impurities by SOP 7040, Rev 10
Inductively Coupled Plasma - Mass Spectrometry

Sample preparation: 0.0142 g of sample was mixed with 2 mL water, 3 mL nitric acid, 0.5 mL hydrochloric acid and internal standard solution, then diluted to 100 g and heated in a hot water bath for 1 hour (the material partially dissolved). The original preparation and a 1:50 dilution were analyzed by ICPMS.

Sample ID: RN

	ppm	Detection Limit		ppm	Detection Limit
Aluminum	110	4	Molybdenum	77	0.2
Antimony	2.2	0.1	Neodymium	ND	0.07
Arsenic	9.0	0.6	Nickel	420	0.2
Barium	ND	0.3	Niobium	ND	0.08
Beryllium	ND	0.07	Osmium	ND	0.4
Bismuth	ND	0.07	Palladium	ND	0.07
Boron	ND	3	Phosphorus	300	60
Bromine	ND	80	Platinum	ND	0.08
Cadmium	ND	0.07	Potassium	ND	200
Calcium	110	30	Praseodymium	ND	0.07
Cerium	ND	0.07	Rhenium	ND	0.07
Cesium	ND	0.07	Rhodium	ND	0.6
Chromium	580	0.6	Rubidium	ND	0.07
Cobalt	25	0.07	Ruthenium	ND	0.07
Copper	270	0.3	Samarium	ND	0.07
Dysprosium	ND	0.09	Selenium	ND	1
Erbium	ND	0.1	Silicon	720	60
Europium	ND	0.07	Silver	0.36	0.1
Gadolinium	ND	0.07	Sodium	ND	100
Gallium	0.81	0.07	Strontium	0.19	0.09
Germanium	9.0	0.4	Tantalum	ND	0.08
Gold	ND	2	Tellurium	ND	0.6
Hafnium	ND	0.07	Thallium	ND	0.7
Holmium	ND	0.07	Thorium	ND	0.07
Iodine	ND	0.1	Thulium	ND	0.07
Iridium	ND	0.6	Tin	28	0.1
Iron	MATRIX		Titanium	ND	1
Lanthanum	ND	0.2	Tungsten	ND	50
Lead	4.9	0.4	Uranium	ND	0.07
Lithium	ND	8	Vanadium	ND	2
Lutetium	ND	4	Ytterbium	ND	0.4
Magnesium	ND	4	Yttrium	ND	0.2
Manganese	1700	0.08	Zinc	19	1
Mercury	ND	1	Zirconium	ND	0.09

Date Analyzed: 08-06-10
Elements Not Analyzed: All Gases, C, S, Sc, In, Tb

Figure 40-Results of ICP-MS Analysis of Metallic Portion of Ron Noel Object

The detected elements are shown, in order of abundance, in Table 1. A total of twenty (20) elements were detected in the sample.

Iron was the most abundant element in the sample, as observed previously in the EDX data. Manganese was a minor component element (0.17%), with silicon (Si, 0.072%), chromium (Cr, 0.058), nickel (Ni, 0.042%), phosphorus (P, 0.030%), copper (Cu, 0.027%), aluminum (Al, 0.011%), and calcium (Ca, 0.011%) as major trace elements.

Minor trace elements included molybdenum (Mo, 77 ppm), tin (Sn, 28 ppm), cobalt (Co, 25 ppm), zinc (Zn, 19 ppm), arsenic (As, 9 ppm), germanium (Ge, 9 pm), lead (Pb, 4.9 ppm), antimony (Sb, 2.2 ppm), gallium (Ga, 0.81 ppm), silver (Ag, 0.36 ppm), and strontium (Sr, 0.19 ppm).

Table 1-Elements Detected in Implant Sample by ICP-MS-in Order of Abundance

Element[2]	Amount (ppm)	Detection Limit (ppm)	Element	Amount (ppm)	Detection Limit (ppm)
Iron	Matrix	NS	Tin	28	0.1
Manganese	1700	0.08	Cobalt	25	0.07
Silicon	720	50	Zinc	19	1
Chromium	580	0.06	Arsenic	9	0.6
Nickel	420	0.2	Germanium	9	0.4
Phosphorus	300	60	Lead	4.9	0.4
Copper	270	0.3	Antimony	2.2	0.1
Aluminum	110	4	Gallium	0.81	0.07
Calcium	110	30	Silver	0.36	0.1
Molybdenum	77	0.2	Strontium	0.19	0.09

Isotopic Analysis

The raw ICP-MS data from which the isotopic ratios of the sample could be calculated are not presently available.

[2] Red denotes major component elements (100%-1%), green-minor component elements (10,000 ppm-1,000 ppm) blue-major trace elements (1,000 ppm-100 ppm), black-minor trace elements (< 100 ppm).

Discussion

The structure of the Ron Noel object was somewhat typical of the objects removed from patients in previous surgeries in that the metallic portion of the object was surrounded by an organic "capsule" of tissue, which was connected to the subject's nervous system.

This object is of a different type than the "John Smith" object which was removed from another patient in the previous surgery. Besides being located in different areas of the body, there were many structural differences between the two objects.

It is likely that the Ron Noel object had a different function than the John Smith object, since the removal of the John Smith object caused only a small difference in Mr. Smith's mood and thought patterns, while the removal of the object from Mr. Noel caused the onset of extreme moodiness and depression. Also, the different locations of the two objects in the subject's bodies, also implies a possible difference in function.

Location in Body: The John Smith (JS) object was located in the left, second toe, while Ron Noel's object (RN) was located in the right hand.

Device Appearance and Characteristics: The JS object was cylindrical, and surrounded by a dark grey, tough, membrane, as seen previously in implants of this general type. This membrane is electrically conductive, and is thought to be the interface between the device and the nervous system.

The RN object was roughly rectangular, and was surrounded by what appeared to be epithelial tissue, which was contained large (30-40 μm) vesicles of a yellow, liquid oil, which was shown by FTIR analysis to have a high concentration of lauric acid. The FTIR spectrum of the oil most closely matched that of coconut oil. It is thought that this oil may be a di, or tri glyceride ester of lauric acid.

Since both coconut oil and lauric acid have antibacterial properties, it is likely that the oil vesicles function to prevent any infection, which could disrupt the connection to the nervous system.

Both devices were connected to the subject's nervous system via proprioceptor nerves. Nerve bundles near the RN device were imaged by light microscopy, shortly after surgical removal.

Pathology reports on both objects showed an anomalous lack of immune response to the presence of the objects in the subject's bodies.

Composition of Objects: Both objects were metallic, and composed mainly of iron. In the case of the JS object, ICP-MS elemental analysis showed about 5% nickel, and trace metals, including gallium, germanium, platinum, and iridium, indicating that the main body of the object was manufactured from meteoric iron.

The JS object also had an exterior coating, which appeared like mother-of-pearl in light microscopy, and had a composition much like a biological hard part, like shell, or bone. EDX analysis indicated that this coating was high in calcium (Ca), silicon (Si), carbon (C), oxygen (O), phosphorus (P), and sulfur (S).

The metallic portion of the RN object also had a coating, which was a black substance that the EDX results indicated was mostly iron oxide, but also contained carbon (C), sodium (Na), aluminum (Al), phosphorus (P), sulfur (S), chlorine (Cl), potassium (K), calcium (Ca), and chromium. This composition is similar to the coating on the John Smith object, except for the much higher concentration of iron oxide, and the presence of chromium (Cr).

ICP-MS analysis indicated that the major component of the RN object was iron (Fe). Very little nickel was detected in the RN object, which precludes the possibility of it being manufactured using meteoric iron as a base material, although the amounts of nickel (Ni), gallium (Ga), and germanium (Ge) detected indicate that perhaps 1% meteoric iron may have been an additive to a base iron alloy material.

The coating on the RN object contained deep pits, approximately 10 μm across, which appeared to go through the coating to the metal. Pits were not visible in the coating of the JS object.

Analysis of the isotopic data provided by the ICP-MS analysis of the JS object showed very skewed isotopic ratios in the material, compared with the known terrestrial elemental isotopic ratios which, if correct, would indicate that the material probably originated outside our solar system. Isotopic data will be obtained on the RN object in the near future.

Presence of Carbon Nanotubes: The JS object was brittle, and broke into several pieces upon removal. The brittleness was later found to be caused by the presence of inclusions, consisting of micron-sized carbon nanotube bundles.

The bundles were coated with a layer of material which was much like the outer coating of the device. These CNT bundles were thought to be carbon nanotube electronics, responsible for the function of the device.

In contrast, the RN object appeared to be of more homogeneous composition, without visible inclusions. It was extremely hard, and could not be cut by a steel razor knife blade, or wire cutters. The object was then taken to a machine shop for cutting; the shop also could not cut the object, and they reported that it had the highest hardness, on the Rockwell hardness scale, and was the hardest material they had ever seen.

The object was then taken to a laser shop, which managed to cut it, using a high-power, pulsed, laser.

Both devices showed carbon nanotube (CNT) spectral signatures on Raman analysis, with the RN object having a stronger CNT Raman signal The CNTs appeared to be single-walled type (SWCNT) with an average diameter of approximately 1 nm.

The SWCNT in the RN object were apparently much better dispersed in the metallic portion of the object than was the case in the JS object, and there were no visible "islands" of SWCNT visible on SEM images anywhere in the metal of the RN object. The increased dispersal of the SWCNT in the metal probably accounts for the extreme mechanical strength of the RN object, and the metal could be thought of as an advanced Iron/CNT metal matrix composite. In this case, the reinforcing CNTs probably also act as the device electronics.

The manufacture of materials such as this are being investigated by Terrestrial materials science, but the research is known to be in its infancy, and the manufacture of a device with this class of materials is beyond the technology of Terrestrial, civilian, science.

The CNT sheets, seen in the acid-etched half of the RN object did show were probably buried in the metal before the acid etch, and were probably the underlying structures which gave rise to the pits in the coating. It is not known whether or not similar sheets of CNT existed further from the surface of the metal.

In addition, wire-like structures, with high carbon content, approximately 10 µm in diameter, were seen in the SEM mages of both samples. These structures are most likely large CNT bundles, and appear to be the main electrical connections to the devices, in both cases.

Other Properties: Both of the objects possessed magnetic fields of approximately 10 mGauss, and gave off radio signals. The RN device was shown to not always be active, while in the subject's body, and radio signals could not always be detected from it.

The pieces of both objects tended to return to their original orientation when placed together, probably due, at least in part, to the magnetic fields given off by the samples.

Conclusions

1) The sample consists mainly of iron, with a high carbon and oxygen content (EDX data). The iron base material contains 0.17% manganese, with significant amounts of silicon, chromium, and nickel, and is highly magnetic. The nickel content is only about $1/100^{th}$ as great as what was detected in the "John Smith" implant, from surgery #15.
2) The nickel content, along with the traces of gallium, and germanium present, strongly suggest that the metallic portion of the sample was manufactured, but contains some meteoric iron.
3) The device contains single-walled carbon nanotubes (SWCNT), as was observed in the John Smith implant; the Raman carbon nanotube signal is, in fact, much higher than was observed in previous implants. The carbon nanotubes appeared to be dispersed in the material much more thoroughly than was the case in the John Smith implant, and no discrete areas of SWCNT were seen.

4) The mechanical strength of the device was unprecedented, indicating that the manufacture of the material of which it is made is well beyond the technology of known science.
5) The function of the device cannot be determined with certainty from the available data, and the device may have had multiple functions and missions. It is likely, however, that two of its functions had to do with monitoring of the physiological state of Mr. Noel's body, and mood/mind control. The possible mood/mind control aspect is highlighted by the extreme depression suffered by Mr. Noel for the first few weeks after the removal of the device.

Appendix

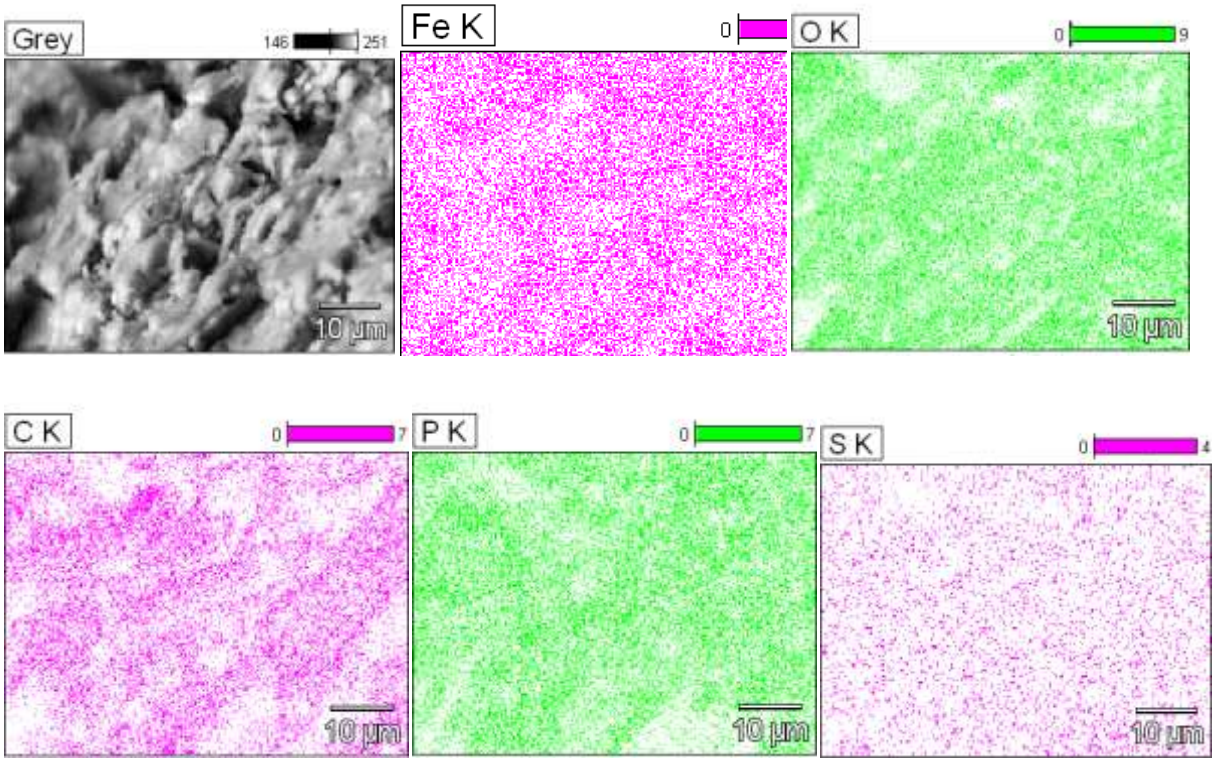

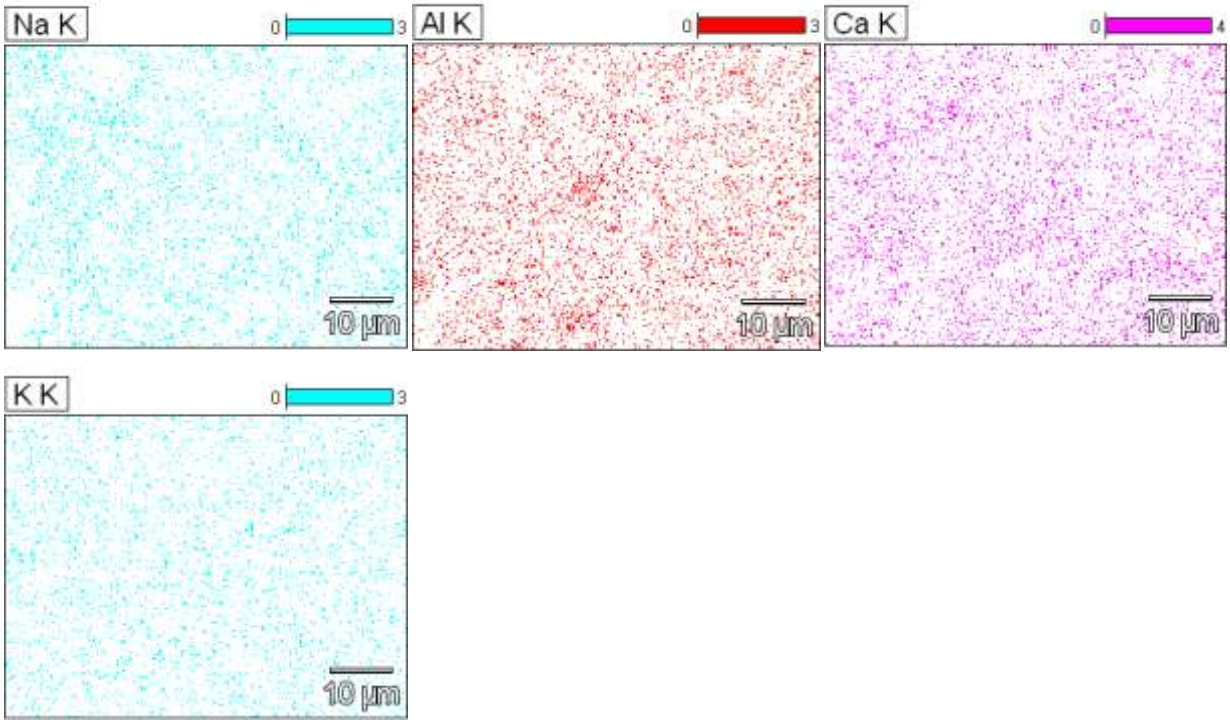

Figure 41-EDX mapping results for Object Coating

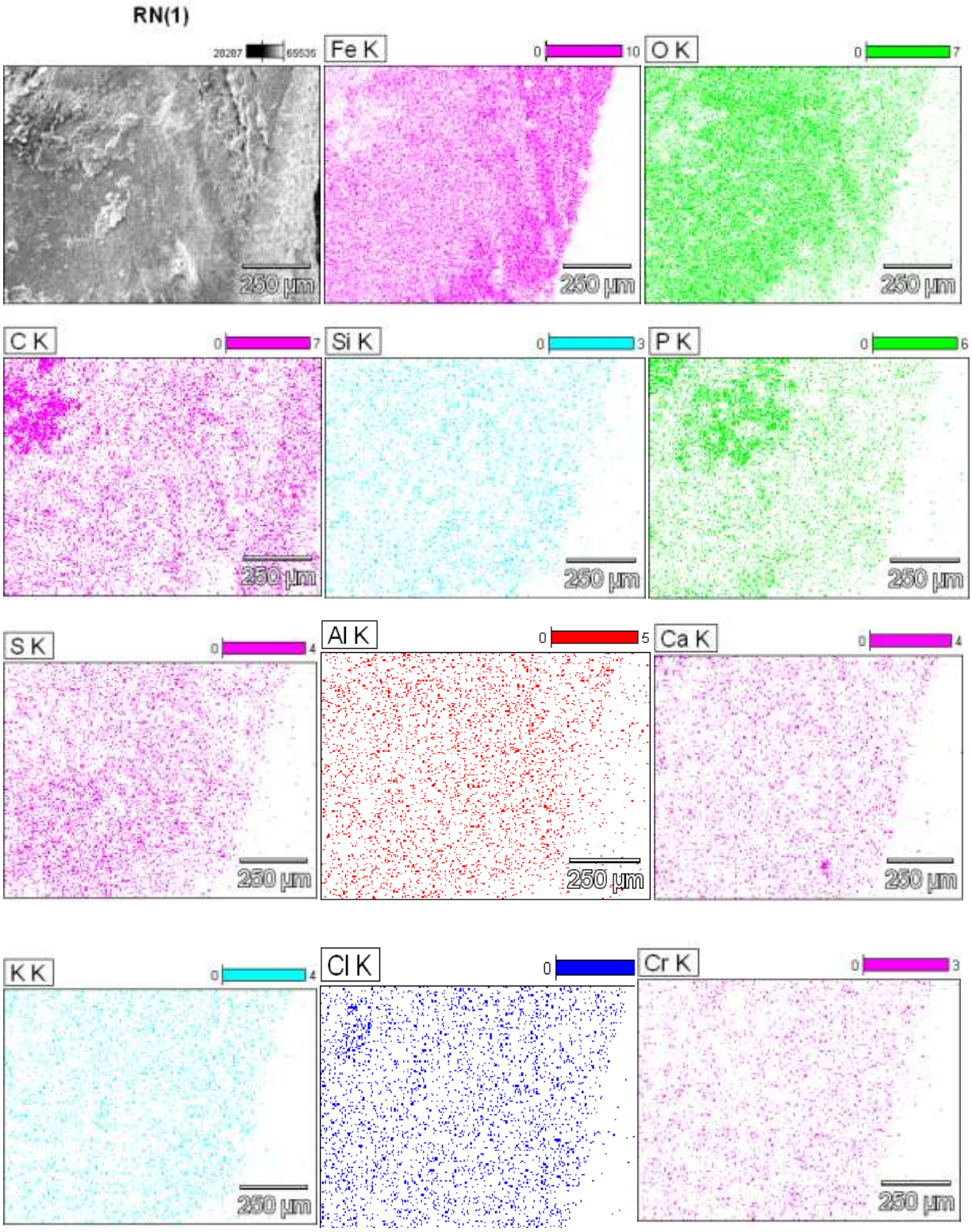

Figure 42- EDX mapping Results for Object Metallic Surface

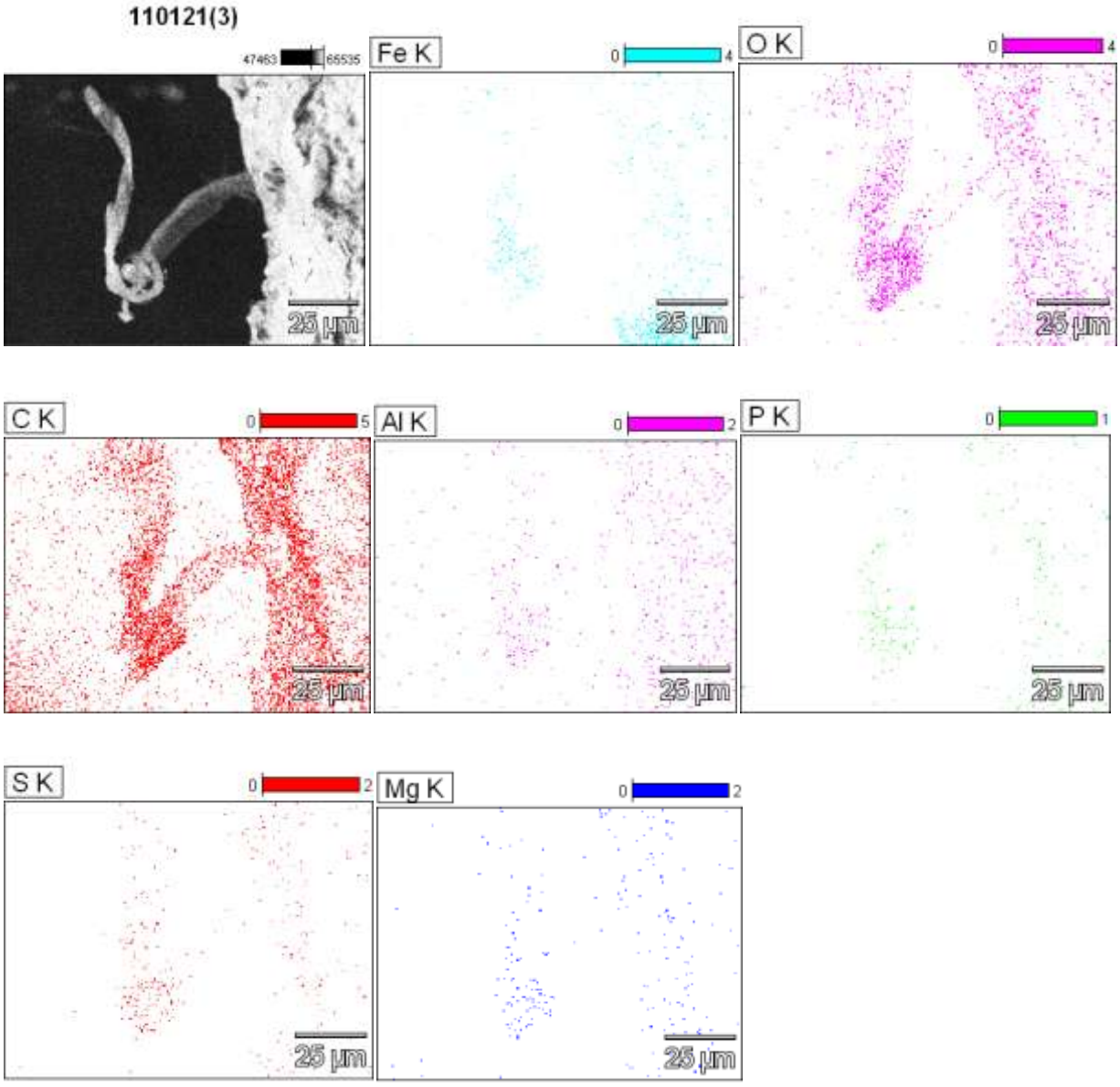

Figure 43- EDX mapping Results for Object Surface-Acid Etched